

Photoelectrochemical behaviour of pulse plated CdS films

K. R. Murali · P. Thirumoorthy · V. Sengodan

Received: 1 November 2007 / Accepted: 11 March 2008 / Published online: 3 April 2008
© Springer Science+Business Media, LLC 2008

Abstract Cadmium sulphide (CdS) films were deposited by the pulse plating technique at room temperature and at different duty cycles in the range of 6–50% using AR grade 0.25 M cadmium sulphate and 0.30 M sodium thiosulphate at a deposition potential of -0.75 V (SCE). The total deposition time was kept constant at 1 h. The thickness of the films were around 2.0 μm . X-ray diffraction (XRD) studies indicate the formation of polycrystalline films with the cubic structure. The crystallite size increased from 23.0 to 27.5 nm as the duty cycle increased from 10 to 50%. Optical absorption studies indicated a direct band gap in the range of 2.40 – 2.80 eV as the duty cycle is decreased. XPS studies indicated the formation of CdS. Photoelectrochemical (PEC) cell measurements made with the photoelectrodes deposited at 50% duty cycle have exhibited higher conversion efficiency compared to earlier reports.

1 Introduction

Extensive research has been done on the deposition and characterization of Cadmium sulphide (CdS) semiconducting

thin films due to their potential application in the area of optoelectronic device fabrication [1–5]. Polycrystalline CdS thin films have good optical transmittance, wide band gap and electrical properties suitable for their application to solar cell fabrication [6], CdS-based solar cell structure exhibits better optical confinement towards higher efficiencies [7–10]. Direct band gap CdS thin films have been the subject of intensive research because of its intermediate band gap, high-absorption coefficient, electron affinity, low resistivity, easy ohmic contact and finally the structure. Reasonable conversion efficiency, stability and availability of low-cost deposition technique attracts the usage of CdS as window electrode in solar cell structure [11]. In recent years, high priority has been given to develop low-cost deposition technique to deposit CdS thin films [12]. Various deposition techniques such as electrodeposition [13], screen printing [14], sputtering [15], spray pyrolysis [16], chemical bath deposition [17], etc., have been reported. In this paper, results of CdS films pulse deposited at different duty cycles in the range of 6–50% are presented and discussed.

2 Experimental techniques

CdS films were deposited by the pulse plating technique at room temperature and at different duty cycles in the range of 6–50% using AR grade 0.25 M cadmium sulphate and 0.30 M sodium thiosulphate at a deposition potential of -0.75 V (SCE). Twenty millilitre of cadmium sulphate and 10 mL of sodium thiosulphate were used for the deposition. Conducting tin oxide substrates (10 ohms sq^{-1}) were employed as substrates. The details of the pulse plating technique is given in an earlier publication [18]. The total deposition time was kept constant at 1 h. The thickness of the films were measured by Mitutoyo surface

K. R. Murali (✉)
Electrochemical Materials Science Division, Central
Electrochemical Research Institute, Karaikudi 630 006, India
e-mail: muraliramkrish@gmail.com

P. Thirumoorthy
Department of Electronics, K.S.R. College of Arts and Science,
Thiruchengode, India

V. Sengodan
S.N.R. Sons College, Coimbatore, India

profilometer and it was found to be around 2.0 μm . Structural studies were made by PANalytical X-ray diffractometer with $\text{CuK}\alpha$ radiation. Optical absorption studies were made on the films deposited on conducting glass substrates using an Hitachi U3400 UV–VIS–NIR spectrophotometer. Atomic force microscopic studies were made with Molecular imaging systems. Photoelectrochemical (PEC) cells were prepared using the films deposited at different duty cycles on titanium substrates heat treated at different temperatures. The films were lacquered with polystyrene in order to prevent the metal substrate portions from being exposed to the redox electrolyte. These films were used as the working electrode. The electrolyte was 1 M polysulphide. This electrolyte was chosen, as it is well known that CdS electrode has reasonable stability and yield respectable outputs in polysulphide. The light source used for illumination was an ORIEL 250 W tungsten halogen lamp. A water filter was introduced between the light source and the PEC cell to cut off the IR portion. The intensity of illumination was measured with a CEL suryamapi, whose readings are directly calibrated in mW cm^{-2} . The intensity of illumination was varied changing the distance between the source and the cell. The power output characteristics of the cells were measured by connecting the resistance box and an ammeter in series and the voltage output was measured across the load resistance. The photocurrent, dark current and output voltage were measured with a HIL digital multimeter.

3 Results and discussion

X-ray diffraction (XRD) pattern of the CdS films deposited at different duty cycles is shown in Fig. 1. The XRD

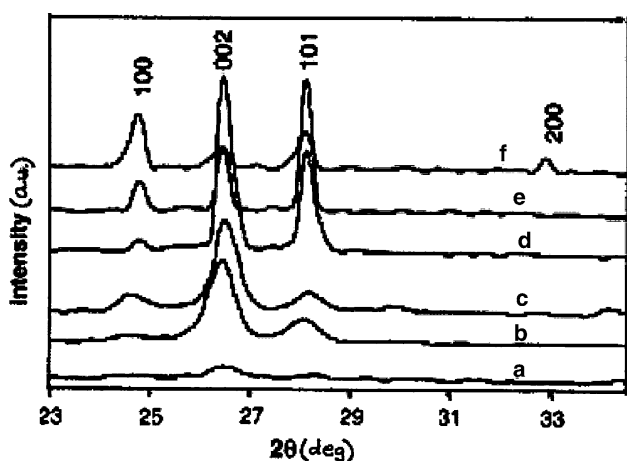


Fig. 1 X-ray diffraction pattern of CdS films deposited at different duty cycles (a) 6%, (b) 10%, (c) 15%, (d) 25%, (e) 33%, (f) 50%

pattern indicates the formation of polycrystalline films with the cubic structure. Peaks corresponding to the (100), (002), (100) and (200) reflections were observed in all the cases. It is observed from the figure that the height of the peaks increase with duty cycle and the width of the peak decreases with increase of duty cycle. For a duty cycle of 6%, the peaks are not well defined and peaks begin to appear only for duty cycles in the range of 10–50%. This is understandable since, at a duty cycle of 6%, the flux of ions are available for a very short time for deposition and the thickness of the film is very small around 0.1 μm . At higher duty cycles, the flux of ions are available for a longer period and hence the thickness increases. The films were post-heat treated at different temperatures in argon atmosphere to induce photoactivity. Figure 2 indicates the XRD patterns of the CdS films deposited at 50% duty cycle and post-treated at different temperatures. It is observed that the crystal structure changes from cubic to hexagonal after heat treatment. The peaks corresponding to (100), (002), (101), (102), (110), (103) and (112) reflections are observed in all cases. The peak corresponding to (101) orientation is found to increase in intensity as the duty cycle increases. The width of the peak also decreases with increase of duty cycle indicating improved crystallinity.

The average grain size and surface roughness of the CdS films deposited at different duty cycles was studied by Atomic force microscopy (AFM). Figure 3 shows the AFM images of the CdS films. It is observed that the surface roughness increases from 14.8 to 19.9 nm as the duty cycle increases. The crystallite size was found to increase from 23.0 to 27.5 nm as the duty cycle increased from 10 to 50% (Fig. 4).

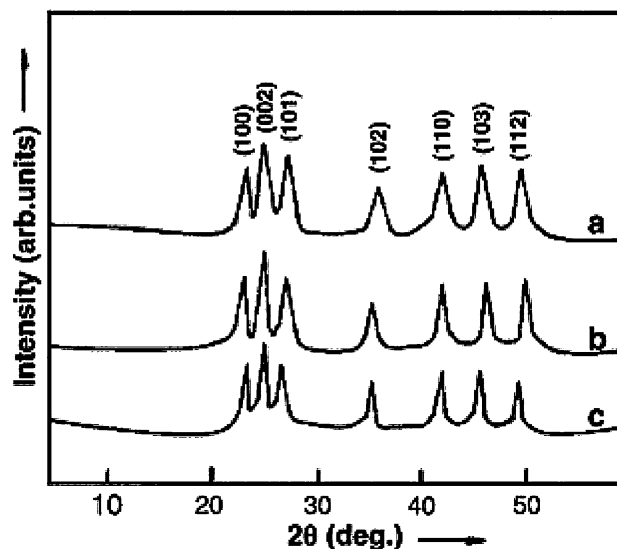


Fig. 2 X-ray diffraction pattern of CdS films deposited at 50% duty cycle and heat treated at different temperatures (a) 450 °C, (b) 500 °C, (c) 550 °C

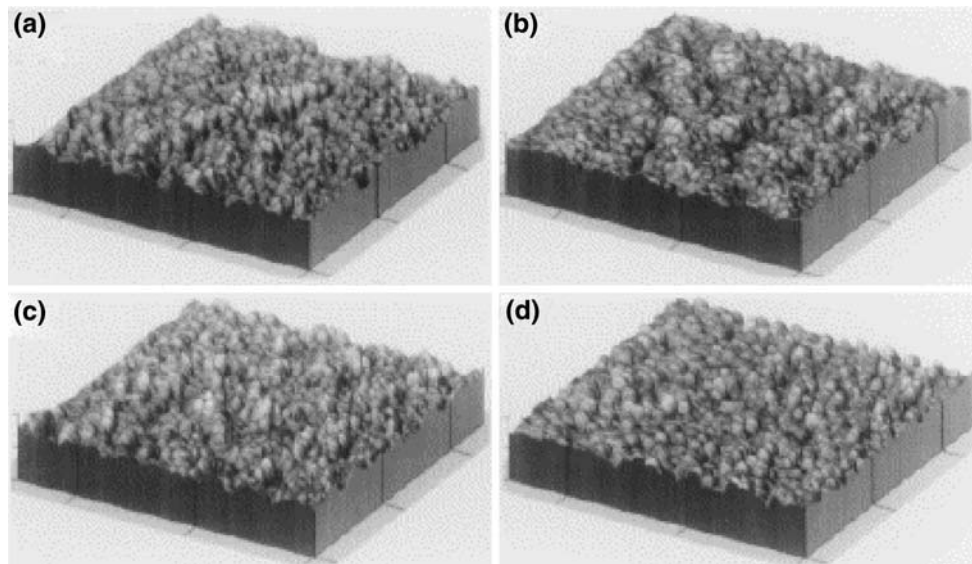


Fig. 3 AFM images of the CdS films deposited at different duty cycles (a) 10%, (b) 25%, (c) 33%, (d) 50%

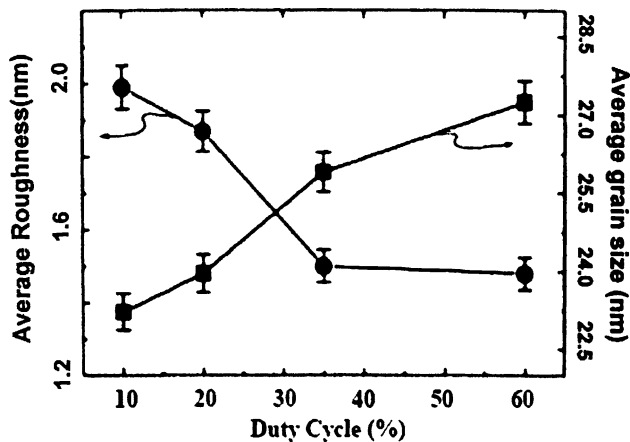


Fig. 4 Average grain size and surface roughness of the CdS films deposited at different duty cycles

Figure 5 shows the XPS spectrum of the CdS films deposited at different duty cycles. Peaks corresponding to S_{2p} and $Cd_{3/2}$ and $Cd_{5/2}$. The peaks are found to increase in intensity with increase of duty cycle. This is in good agreement with the literature values [19]. Figure 6 shows the plot of $(\alpha h\nu)^2$ vs. $h\nu$ for the above films. The plot is linear indicating the direct band gap nature of the films. Extrapolation of the line to the $h\nu$ axis indicated a direct band gap in the range of 2.40–2.80 eV as the duty cycle is decreased. This is due to the decrease in particle size with decrease of duty cycle. The variation of band gap at different duty cycles is due to the variation of crystallite size with duty cycle. Strong and weak confinements were noticed for the films. For strong confinement, the exciton energy is given by,

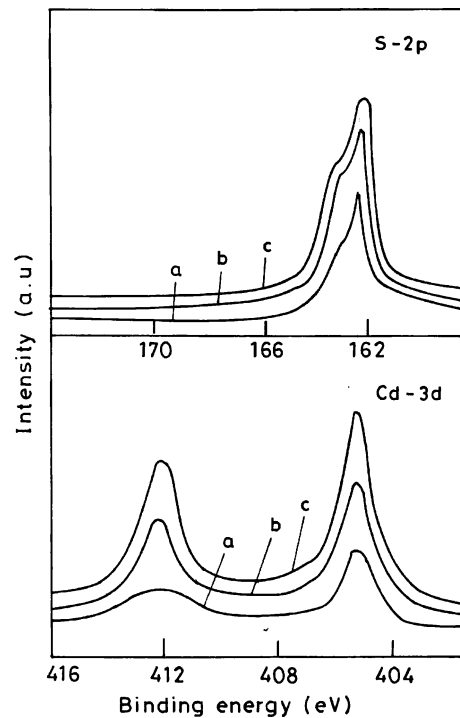


Fig. 5 XPS spectrum of the CdS films deposited at different duty cycles (a) 10% (b) 25% (c) 50%

$$E_s = E_g + \frac{h^2 \pi^2}{2\mu^2} - \frac{1.786 \cdot e^2}{4\pi \cdot R \epsilon_0 \epsilon} - 0.248 E_{Ry}^*$$

where E_g is the band gap of bulk CdS, the second term is related to the quantum localization energy, the third term represents the Coloumb energy and the fourth term represents the correlation energy in which E_{Ry}^* is the effective Rydberg energy and can be written as

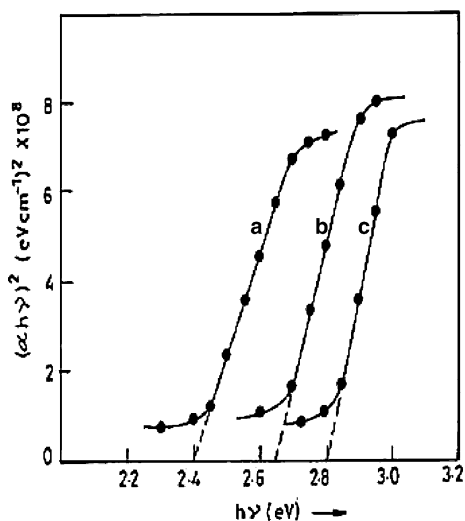


Fig. 6 $(\alpha ch\nu)^2$ vs. $h\nu$ plot for the CdS films deposited at different duty cycles (a) 50% (b) 33% (c) 10%

$$\left\{ \frac{\mu \cdot e^4}{2(4\pi\epsilon_0\epsilon)^2 h^2} \right\}$$

where μ is the reduced effective mass, ϵ is the dielectric constant for CdS and ϵ_0 is the permittivity of free space. The estimated band gap of 2.80 eV due to strong confinement matches with the band gap value obtained from absorption measurements for the films deposited with 10% duty cycle. PEC cells were prepared using the films deposited at different duty cycles on titanium substrates heat treated at different temperatures. The electrolyte was 1 M polysulphide (1 M Na_2S , 1 M S and 1 M NaOH). The CdS photoelectrodes were dipped in the electrolyte and allowed to attain equilibrium under dark conditions for about 10 min. The dark current and voltage values were noted. The cells were then illuminated by the light source and the current and voltage were measured for each setting of the resistance box. The photocurrent and photovoltage were calculated as the difference between the current under illumination and the dark current, and voltage under illumination and dark voltage respectively. The photoelectrodes deposited at 50% duty cycle exhibited maximum photoactivity, hence further studies were carried out on these samples. The power output characteristics of the PEC cells made using the photoelectrodes deposited at 50% duty cycle and post-heat treated at different temperatures is shown in Fig. 7. From the figure, it is observed that the PEC output parameters, viz., open circuit voltage and short circuit current were found to increase for the electrodes heat treated up to a temperature of 525 °C. Photoelectrodes heat treated at temperatures greater than this value exhibited lower open circuit voltage and short circuit current due to the reduction in thickness of the films as well as the

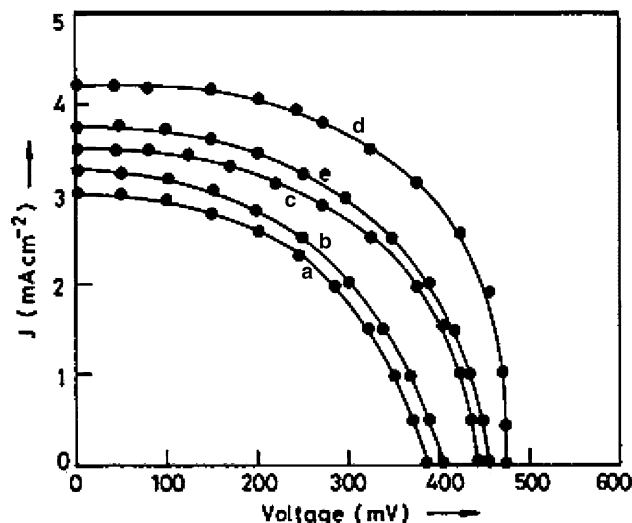


Fig. 7 Power output characteristics of the CdS photoelectrodes deposited at 50% duty cycle and post-heat treated at different temperatures (a) 450 °C (b) 475 °C (c) 500 °C (d) 525 °C (e) 550 °C

slight change in stoichiometry. Hence, further studies were made only on the films heat treated at 525 °C. The power output characteristics of the electrodes heat treated at 525 °C were studied at different intensities of illumination in the range of 20–100 mW cm^{-2} . It was observed that both V_{oc} and J_{sc} increased with increase of intensity. V_{oc} increased from 0.23 to 0.50 V as intensity increased from 20 to 100 mW cm^{-2} . Beyond 80 mW cm^{-2} illumination, V_{oc} was found to saturate as is commonly observed in the case of photovoltaic cells and PEC cells [20]. J_{sc} is found to increase linearly with intensity of illumination.

The effect of photoetching on the PEC performance was studied by shorting the photoelectrode and the graphite counter electrode under an illumination of 100 mW cm^{-2} in 1:100 HCl for different durations in the range of 0–100 s. Both photocurrent and photovoltage are found to increase up to 80 s photoetch, beyond which they begin to decrease. Photoetching leads to selective attack of surface states not accessible to chemical etchants. It is observed that during photoetching, the open circuit voltage and short circuit current increase from 0.45 to 0.65 V and from 4.0 to 7.8 mA cm^{-2} , respectively, for an intensity of 80 mW cm^{-2} . The decrease in the voltage and current beyond 80 s photoetching can be attributed to increase in surface area due to prolonged photoetching [21]. The power output characteristics (Fig. 6) after 80 s photoetching indicates a V_{oc} of 0.60 V, J_{sc} of 7.50 mA cm^{-2} , ff of 0.53 and η of 3.0% for 80 mW cm^{-2} illumination. The photovoltaic parameters of the electrodes with and without photoetching are shown in Table. 1. The efficiency of the photoelectrodes is higher than the earlier reports [22–24]. Spectral response measurements were carried out on the photoelectrodes by using photophysics monochromator and a 250 W tungsten

Table 1 Photovoltaic parameters of CdS photoelectrodes deposited at 50% duty cycle and post-heated at different temperatures in Argon (Intensity of illumination—80 mW cm⁻²)

Temperature of heat treatment (°C)	V _{oc} (V)	J _{sc} (mA cm ⁻²)	ff	η (%)	R _s (Ω)	R _{sh} (kΩ)
450	0.26	1.8	0.56	0.33	50.0	2.50
475	0.30	2.6	0.68	0.66	20.0	2.00
500	0.375	3.0	0.67	0.93	18.0	3.60
525	0.475	4.30	0.56	1.43	10.0	5.00
550	0.450	3.55	0.60	1.20	15.0	2.80
525 (After photoetch)	0.600	7.50	0.53	3.00	13.0	2.00

halogen lamp, 1 M polysulphide as electrolyte, graphite as counter electrode and the photoelectrode as the working electrode. The wavelength was varied in the range of 400–900 nm and the photocurrent was noted at each wavelength. The photocurrent value were used for the calculation of the quantum efficiency (Φ) using the well-known equation [25],

$$\Phi = \frac{1240 \cdot J_{sc}}{\lambda \cdot P_{in}}$$

where, J_{sc} is the photocurrent, λ is the wavelength of illumination, P_{in} is the power of the light incident on the photoelectrode. Plot of Φ vs. λ for the CdS electrode deposited at 50% duty cycle and post-heat treated at 525 °C is shown in Fig. 8. The value of Φ_{max} occurs at 525 nm corresponding to the band gap of 2.36 eV. This value matches well with the band gap value of 2.39 eV estimated from optical absorption measurements.

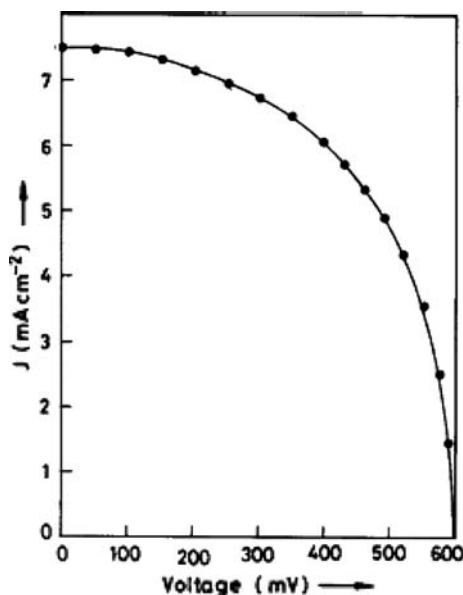


Fig. 8 Power output characteristics of the CdS photoelectrodes deposited at 50% duty cycle and post-heat treated at 525 °C after photoetching for 80 s

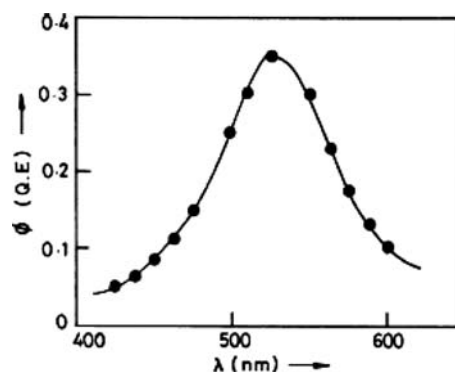


Fig. 9 Quantum efficiency vs. wavelength plot of the CdS photoelectrodes deposited at 50% duty cycle and post-heat treated at 525 °C

4 Conclusions

The results of this study clearly indicate that CdS films with crystallite size in the range of 15–60 nm can easily be prepared by the pulse plating technique. CdS photoelectrodes with higher photo-outputs compared to earlier reports on thin film photoelectrodes are obtained by this technique. Further work aims at deposition of large area electrodes (Fig. 9).

References

- G.C. Morris, R. Vanderveen, Sol. Energy Mater. Sol. Cells **27**, 305 (1992)
- T.L. Chu, S.S. Chu, N. Schultz, C. Wang, C.Q. Wu, J. Electrochem. Soc. **139**, 2443 (1992)
- I. Markov, E. Valova, M. Ilieva, I. Krstev, J. Cryst. Growth **65**, 611 (1983)
- Y.Y. Ma, R.H. Bube, J. Electrochem. Soc. **124**, 1430 (1977)
- P.C. Pande, G.J. Russell, J. Woods, Thin Solid Films **121**, 85 (1984)
- T.L. Chu, S.S. Chu, J. Britt, C. Ferekides, C. Wang, C.Q. Wu, H.S. Ullal, IEEE Electron Device Lett. **13**, 303 (1992)
- J.L. Shay, S. Wagner, M. Bettini, K.J. Bachman, E. Buchler, J. Appl. Phys. **24**, 483 (1977)
- R.W. Birkmire, B.E. Mc Candles, W.N. Shafarman, Sol. Cells **23**, 115 (1988)
- Y.S. Tyan, Sol. Cells **23**, 59 (1988)
- P.V. Mayer, Sol. Cells **23**, 59 (1988)
- G. Morris, Proceedings of the Workshop on Low Cost Electronic Materials and Solar Cells, Columbu, Srilanka, 1997, p. 35
- D. Bonnet, H. Richter, K.H. Jager, Proceedings of 13th European Photovoltaic Solar Energy Conference France, 23–24, October 1995, p. 1456
- S. Chaure, N.B. Chaure, R.K. Pandey, J. Nanosci. Nanotechnol. **7**, 945 (2007)
- I. Clemminck, M. Burgelman, M. Casteleyn, B. Depuydt, Int. J. Sol. Energy **12**, 67 (1992)
- B.S. Moon, J.H. Lee, H. Jung, Thin Solid Films **511**, 299 (2006)
- D.R. Acosta, C.R. Magana, A.I. Martinez, A. Maldonado, Sol. Energy Mater. Sol. Cells **82**, 11 (2004)
- B. Pradhan, A.K. Sharma, A.K. Ray, J. Cryst. Growth **304**, 388 (2007)

18. K.R. Murali, M. Balasubramanian, *Mater. Sci. Eng. A* **431**, 118 (2006)
19. J.S. Hammond, S.W. Gaarenstroom, N. Winograd, *Anal. Chem.* **47**, 2194 (1975)
20. J.P. Mangalhara, R. Thangaraj, O.P. Agnihotri, *Bull. Mater. Sci.* **10**, 333 (1988)
21. G. Hodes, *Nature* **285**, 29 (1980)
22. R.C. Bharadwaj, C.M. Jadhav, M.M. Taqui Khan, *Sol. Cells* **12**, 71 (1984)
23. M. Neumann Spallart, K. Kalyanasundaram, *Ber. Bunsenges. Phys. Chem.* **85**, 1112 (1981)
24. Y. Ramprakash, V. Subramanian, R. Krishnakumar, A.S. Lakshmanan, V.K. Venkatesan, *J. Power Sources* **24**, 41 (1988)
25. J. Segui, S. Hot Chandani, D. Baddau, R.M. Leblanc, *J. Phys.* **94**, 8807 (1991)